Engineering Solid Mechanics 9 (2021) 415-424

Contents lists available at GrowingScience

Engineering Solid Mechanics

homepage: www.GrowingScience.com/esm

# Setting up the braking force measurement system of the tractor semi-trailer

**Nguyen Thanh Tung**[a*]

[a]*Vinh Long University of Technology Education, 73, Nguyen Hue Street, Vinh Long city, Vietnam*

**A R T I C L E I N F O**

*Article history*:
Received 10 January 2021
Accepted 3 June 2021
Available online
3 June 2021

*Keywords*:
*Measurement system*
*Experiment*
*Simulation*
*Braking force*
*Tractor semi-trailer*

**A B S T R A C T**

The braking force of the tractor semi-trailer depends on many random factors and road parameters. Therefore, determining the braking force based on theoretical calculation or simulation is not accurate. This paper presents the method of setting up the braking force measurement system of the tractor semi-trailer on the road and constructing the braking dynamics model of the tractor semi-trailer to investigate the braking force using Matlab-Simulink software. The study results show that the average error between the simulation and experimental results of the tractor semi-trailer braking force is 9,81%.

© 2021 Growing Science Ltd. All rights reserved.

**Nomenclature**

| **Symbols** | **Units** | **Definition** |
|---|---|---|
| I | | Axle number of the tractor semi-trailer, i = 1÷6 |
| J | | j = 1, left wheel; j = 2, right wheel; j = 1÷2 |
| $x_{c1}, y_{c1}, z_{c1}$ | m | Displacement in the $B(C_1x_{c1}y_{c1}z_{c1})$ coordinate system |
| $x_{c2}, y_{c2}, z_{c2}$ | m | Displacement in the $B(C_2x_{c2}y_{c2}z_{c2})$ coordinate system |
| $\varphi_{ij}$ | rad | Rotation angle of the ij wheel |
| $\varphi_{c1}$ | Degree | Rotation angle of the tractor body around the $y_{c1}$ axis |
| $\beta_{c1}$ | Degree | Rotation angle of the tractor body around the $x_{c1}$ axis |
| $\psi_{c1}$ | Degree | Rotation angle of the tractor body around the $z_{c1}$ axis |
| $\varphi_{c2}$ | Degree | Rotation angle of the Semi-trailer body around the $y_{c2}$ axis |
| $\beta_{c2}$ | Degree | Rotation angle of the Semi-trailer body around the $x_{c2}$ axis |
| $\psi_{c2}$ | Degree | Rotation angle of the Semi-trailer body around the $z_{c2}$ axis |
| $\alpha_{ij}$ | Degree | Sideslip angle of the ij wheel |
| $s_{xij}$ | | Longitudinal slip ratio of the ij wheel |
| $\varphi_{xij}$ | | Longitudinal friction coefficient of the ij wheel |
| $\varphi_{yij}$ | | Lateral friction coefficient of the ij wheel |
| $m_{c1}$ | kg | Sprung mass of the tractor |
| $m_{c2}$ | kg | Sprung mass of the Semi-trailer |
| $m_{Ai}$ | kg | Un-sprung mass of the ij axle |

* Corresponding author.
E-mail addresses: tungnt@vlute.edu.vn (N. T. Tung)

© 2021 Growing Science Ltd. All rights reserved.
doi: 10.5267/j.esm.2021.6.001

| | | |
|---|---|---|
| $J_x$ | $kgm^2$ | Moment of inertia about the x-axis of the sprung mass |
| $J_y$ | $kgm^2$ | Moment of inertia about the y-axis of the sprung mass |
| $J_z$ | $kgm^2$ | Moment of inertia about the x-axis of the sprung mass |
| $J_{Ayij}$ | $kgm^2$ | Moment of inertia about the y-axis of the ij wheel |
| $F_{Cij}$ | N | The suspension elastic force of the ij wheel |
| $F_{Kij}$ | N | The suspension damping force of the ij wheel |
| $F_{CLij}$ | N | The tire elastic force of the ij wheel |
| $F_{xij}$ | N | The longitudinal force or forward force of the ij wheel |
| $F_{yij}$ | N | The lateral force of the ij wheel |
| $F_{zij}$ | N | The normal force or vertical force or wheel load of the ij wheel |
| $F_{Gij}$ | N | The static weight of the ij wheel |
| $M_{Aij}$ | Nm | The driving torque of the ij wheel |
| $M_{Bij}$ | Nm | The braking torque of the ij wheel |

## 1. Introduction

For braking dynamics of the tractor semi-trailer, both simulation and experimental methods are often used (Tung et al., 2020, Rajamani, 2011; Jazar, 2017; Van-Huong 2014). The simulation method shows the general rule and the physical relationship among parameters quickly and inexpensively. The experimental method shows the values of the parameters in actual and random motion conditions on the road (Chen et al., 2016; Jazar, 2019; Mitschke & Wallentowitz, 1972). However, the experimental method requires the test on road and equipment, which is expensive. Setting up the braking force measurement system of the tractor semi-trailer on the road is a real industrial and safety need all over the world. Hence, there are many research works regarding the experimental measurement, mathematical simulation and dynamic modeling of braking force systems (Werner, 2007; Suh et al., 2000; Bayan et al., 2009; Gäfvert & Lindgärde, 2004; Verma et al., 1980; Zhou et al., 2011; Zhiwei et al., 2005; Guan et al., 2004; Limpert, 1971; Zheng, 2015; Li et al., 2014, 2019; Vincent & Krauter, 1973; Lee et al., 1999; Tianjun & Changfu, 2009; Sampson, 2000). In this research the braking dynamics model of the tractor semi-trailer and its related braking force was simulated and investigated using Matlab-Simulink software and the results of the simulations were compared with the experimental results. The movement of tractor semi-trailer is affected by the tire forces. The tire forces are determined by a tire model (Rajamani 2011, Jazar 2017, Van-Huong 2014). Nowadays, there are many types of tire models such as (i) HSRI (Highway Safety Research Institute) tire model, (ii) Ammon tire model, (iii) Burckhard tire model, (iv) Dugoff tire model, (v) Paceijka tire model and etc. (Paceijka 2002, Mitschke & Wallentowitz1972; Ammon 1997). In this paper, Ammon tire model was selected to determine the tire forces.
According to Ammon tire model, we have formulas to determine tire forces as (Ammon 1997):

$$F_x(s_x,\alpha)=\varphi_{x,max}\frac{\sqrt{s_x^2+\alpha^2}}{s_x}F_z(t)f\left(\frac{\sqrt{s_x^2+\alpha^2}}{s_{x,max}\varphi_{x,max}}\right) \tag{1}$$

$$F_y(s_x,\alpha)=\varphi_{y,max}\frac{\sqrt{s_x^2+\alpha^2}}{\alpha}F_z(t)f\left(\frac{\sqrt{s_x^2+\alpha^2}}{\alpha_{x,max}\varphi_{y,max}}\right) \tag{2}$$

## 2. Theoretical basis

The braking dynamics diagram of the tractor semi-trailer and the wheel dynamics diagram when braking is shown in Fig. 1. This model has also been illustrated in more details in previous works (Rajamani, 2011; Jazar, 2017; Chen et al., 2015). With the use of the method of separating the structure and the Newton-Euler system of equations, the system of the braking dynamics equations of the tractor semi-trailer in the road plane (i.e. XOY) was established as follows (Rajamani, 2011; Jazar, 2017; Tung, 2016):

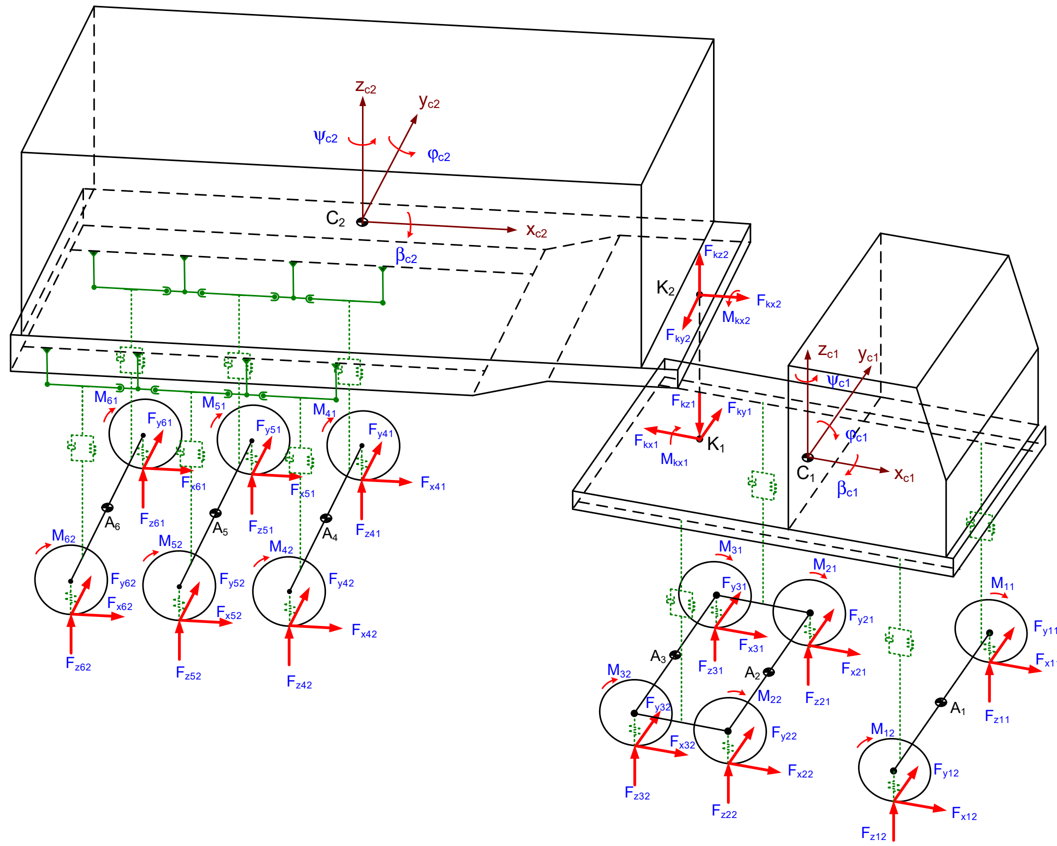


**Fig. 1.** The braking dynamics diagram of the tractor semi-trailer

$$(m_{c1}+\sum_{1}^{3} m_{Ai})(\ddot{x}_{c1}-\dot{\psi}_{c1}\dot{y}_{c1}) = F_{x11}\cos\delta_{11}+F_{x12}\cos\delta_{12}-F_{y11}\sin\delta_{11}-F_{y12}\sin\delta_{12}+(F_{x2j}+F_{x3j})-F_{wx1}-F_{kx1} \tag{3}$$

$$(m_{c1}+\sum_{1}^{3} m_{Ai})(\ddot{y}_{c1}+\dot{\psi}_{c1}\dot{x}_{c1}) = F_{x11}\sin\delta_{11}+F_{x12}\sin\delta_{12}+F_{y11}\cos\delta_{11}+F_{y12}\cos\delta_{12}+(F_{y2j}+F_{y3j})-F_{ky1} \tag{4}$$

$$J_{zc1}\ddot{\psi}_{c1} = [F_{x1j}\sin\delta_{1j}+F_{y1j}\cos\delta_{1j}]l_1+F_{ky1}l_{k1}-F_{y2j}l_2+(F_{x12}\cos\delta_{12}-F_{x11}\cos\delta_{11})b_1+(F_{x32}-F_{x31})b_3-F_{y3j}l_3$$
$$+(F_{y11}\sin\delta_{11}-F_{y12}\sin\delta_{12})l_1+(F_{x22}-F_{x21})b_2 \tag{5}$$

$$(m_{c2}+\sum_{4}^{6} m_{Ai})(\ddot{x}_{c2}-\dot{\psi}_{c2}\dot{y}_{c2}) = F_{x4j}+F_{x5j}+F_{x6j}+F_{kx2} \tag{6}$$

$$(m_{c2}+\sum_{4}^{6} m_{Ai})(\ddot{y}_{c2}+\dot{\psi}_{c2}\dot{x}_{c2}) = F_{ky2}+F_{y4j}+F_{y5j}+F_{y6j} \tag{7}$$

$$J_{zc2}\ddot{\psi}_{c2} = (F_{x42}-F_{x41})b_4+(F_{x52}-F_{x51})b_5+(F_{x62}-F_{x61})b_6+F_{ky2}l_{k2}-F_{y4j}l_4-F_{y5j}l_5-F_{y6j}l_6 \tag{8}$$

The dynamics equations of the tractor semi-trailer in the longitudinal plane (XOZ) are as follows:

$$m_{c1}(\ddot{z}_{c1}-\dot{\varphi}_{c1}\dot{x}_{c1}) = F_{Cij}+F_{Kij}-F_{kz1} \quad (i=1\div 3) \tag{9}$$

$$m_{c2}(\ddot{z}_{c2}-\dot{\varphi}_{c2}\dot{x}_{c2}) = F_{Cij}+F_{Kij}-F_{kz} \quad (i=4\div 6) \tag{10}$$

$$J_{yc1}\ddot{\varphi}_{c1} = -(F_{C1j}+F_{K1j})l_1+F'_{x1j}(h_{c1}-r_1)+F_{kx1}(h_{c1}-h_{k1})+F_{kz1}l_{k1}+M_{1j} \tag{11}$$

$$J_{yc2}\ddot{\varphi}_{c2} = -(F_{C2j}+F_{K2j})l_2+F'_{x2j}(h_{c2}-r_2)+F_{kx2}(h_{c2}-h_{k2})+F_{kz2}l_{k2}+M_{2j} \tag{12}$$

With i=1…6, j=1 indicating the left wheel, j=2 indicating the right wheel, the dynamics equations of the tractor semi-trailer in the plane (YOZ) are written as follows (Rajamani, 2011; Jazar, 2017; Tung, 2016):

$$J_{xc1}\ddot{\beta}_{c1} = \sum_{i=1}^{i=6}(F_{C2i}+F_{K2i}-F_{C1i}-F_{K1i})w_i+\sum_{i=1}^{i=6}F_i(h_c-h_{Bi})-M_{kx1} \tag{13}$$

$$J_{xc2}\ddot{\beta}_{c2}=\sum_{i=1}^{i=6}(F_{C2i}+F_{K2i}-F_{C1i}-F_{K1i})w_i+\sum_{i=1}^{i=6}F_i(h_c-h_{Bi})-M_{kx2} \tag{14}$$

$$(m_{c1}+\sum_{1}^{3}m_{Ai})(\ddot{x}_{c1}-\dot{\psi}_{c1}\dot{y}_{c1})=F_{x11}cos\delta_{11}+F_{x12}cos\delta_{12}-F_{y11}\sin\delta_{11}-F_{y12}\sin\delta_{12}+(F_{x2j}+F_{x3j})-F_{wx1}-F_{kx1} \tag{15}$$

$$(m_{c1}+\sum_{1}^{3}m_{Ai})(\ddot{x}_{c1}-\dot{\psi}_{c1}\dot{y}_{c1})=F_{x11}cos\delta_{11}+F_{x12}cos\delta_{12}-F_{y11}\sin\delta_{11}-F_{y12}\sin\delta_{12}+(F_{x2j}+F_{x3j})-F_{wx1}-F_{kx1} \tag{16}$$

$$m_{A3}(\ddot{z}_{A3}+\dot{\beta}_{A3}\dot{y}_{A3})=F_{CL3j}+F_{KL3j}-F_{C3j}-F_{K3j} \tag{17}$$

$$m_{A4}(\ddot{z}_{A4}+\dot{\beta}_{A4}\dot{y}_{A4})=F_{CL4j}+F_{KL4j}-F_{C4j}-F_{K4j} \tag{18}$$

$$m_{A5}(\ddot{z}_{A5}+\dot{\beta}_{A5}\dot{y}_{A5})=F_{CL5j}+F_{KL5j}-F_{C5j}-F_{K5j} \tag{19}$$

$$m_{A6}(\ddot{z}_{A6}+\dot{\beta}_{A6}\dot{y}_{A6})=F_{CL6j}+F_{KL6j}-F_{C6j}-F_{K6j} \tag{20}$$

$$m_{A1}(\ddot{y}_{A1}-\dot{\beta}_{A1}\dot{z}_{A1})=F_1+F_{y1j} \tag{21}$$

$$m_{A2}(\ddot{y}_{A2}-\dot{\beta}_{A2}\dot{z}_{A2})=F_2+F_{y2j} \tag{22}$$

$$m_{A3}(\ddot{y}_{A3}-\dot{\beta}_{A3}\dot{z}_{A3})=F_3+F_{y3j} \tag{23}$$

$$m_{A4}(\ddot{y}_{A4}-\dot{\beta}_{A4}\dot{z}_{A4})=F_4+F_{y4j} \tag{24}$$

$$m_{A5}(\ddot{y}_{A5}-\dot{\beta}_{A5}\dot{z}_{A5})=F_5+F_{y5j} \tag{25}$$

$$m_{A6}(\ddot{y}_{A6}-\dot{\beta}_{A6}\dot{z}_{A6})=F_6+F_{y6j} \tag{26}$$

$$J_{Ax1}\ddot{\beta}_{A1}=(F_{C11}+F_{K11}-F_{C12}-F_{K12})w_1-F_{y1j}(r_{1j}+\xi_{A1j})+(F_{CL12}+F_{KL12}-F_{CL11}-F_{KL11})b_1+F_1(h_{B1}-r_1) \tag{27}$$

$$J_{Ax2}\ddot{\beta}_{A2}=(F_{C21}+F_{K21}-F_{C22}-F_{K22})w_2-F_{y2j}(r_{2j}+\xi_{A2j})+(F_{CL22}+F_{KL22}-F_{CL21}-F_{KL21})b_2+F_2(h_{B2}-r_2) \tag{28}$$

$$J_{Ax3}\ddot{\beta}_{A3}=(F_{C31}+F_{K31}-F_{C32}-F_{K32})w_3-F_{y3j}(r_{3j}+\xi_{A3j})+(F_{CL32}+F_{KL32}-F_{CL31}-F_{KL31})b_3+F_3(h_{B3}-r_3) \tag{29}$$

$$J_{Ax4}\ddot{\beta}_{A4}=(F_{C41}+F_{K41}-F_{C42}-F_{K42})w_4-F_{y4j}(r_{4j}+\xi_{A4j})+(F_{CL42}+F_{KL42}-F_{CL41}-F_{KL41})b_4+F_4(h_{B4}-r_4) \tag{30}$$

$$J_{Ax5}\ddot{\beta}_{A5}=(F_{C51}+F_{K51}-F_{C52}-F_{K52})w_5-F_{y5j}(r_{5j}+\xi_{A5j})+(F_{CL52}+F_{KL52}-F_{CL51}-F_{KL51})b_5+F_5(h_{B5}-r_5) \tag{31}$$

$$J_{Ax6}\ddot{\beta}_{A6}=(F_{C61}+F_{K61}-F_{C62}-F_{K62})w_6-F_{y6j}(r_{6j}+\xi_{A6j})+(F_{CL62}+F_{KL62}-F_{CL61}-F_{KL61})b_6+F_6(h_{B6}-r_6) \tag{32}$$

The dynamic model of the wheel is shown in Fig. 2. The dynamic equation of the wheels in the longitudinal plane (XOZ) is written as follows (Rajamani, 2011; Jazar, 2017; Tung, 2016):

$$J_{Ayij}\ddot{\varphi}_{ij}=M_{Aij}-M_{Bij}-F_{xij}r_{dij} \tag{33}$$

$$J_{Ayij}\ddot{\varphi}_{ij}=M_{Aij}-M_{Bij}-F_{xij}r_{dij} \tag{34}$$

$$J_{Ayij}\ddot{\varphi}_{ij}=M_{Aij}-M_{Bij}-F_{xij}r_{dij} \tag{35}$$

$$J_{Ayij}\ddot{\varphi}_{ij}=M_{Aij}-M_{Bij}-F_{xij}r_{dij} \tag{36}$$

$$J_{Ayij}\ddot{\varphi}_{ij}=M_{Aij}-M_{Bij}-F_{xij}r_{dij} \tag{37}$$

$$J_{Ayij}\ddot{\varphi}_{ij}=M_{Aij}-M_{Bij}-F_{xij}r_{dij} \tag{38}$$

$$J_{Ayij}\ddot{\varphi}_{ij}=M_{Aij}-M_{Bij}-F_{xij}r_{dij} \tag{39}$$

$$J_{Ayij}\ddot{\varphi}_{ij}=M_{Aij}-M_{Bij}-F_{xij}r_{dij} \tag{40}$$

$$J_{Ayij}\ddot{\varphi}_{ij}=M_{Aij}-M_{Bij}-F_{xij}r_{dij} \tag{41}$$

$$J_{Ayij}\ddot{\varphi}_{ij}=M_{Aij}-M_{Bij}-F_{xij}r_{dij} \tag{42}$$

$$J_{Ayij}\ddot{\varphi}_{ij}=M_{Aij}-M_{Bij}-F_{xij}r_{dij} \tag{43}$$

$$J_{Ayij}\ddot{\varphi}_{ij}=M_{Aij}-M_{Bij}-F_{xij}r_{dij} \tag{44}$$

The braking force of the tractor semi-trailer is determined from (Chen et al., 2016; Jazar, 2019; Tung, 2016):

$$F_X=(m+m_A)\ddot{x}-F_w \tag{45}$$

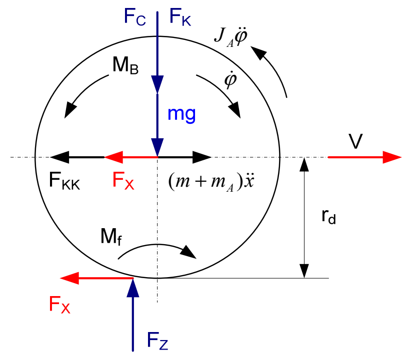


**Fig. 2.** Dynamics of the wheels

## 3. Experiment and simulation

### *3.1. Setting up the measurement system*

To determine the braking force of the tractor semi-trailer, the following basic parameters are required to be known: Measure the wheel angular velocity ($\dot{\varphi}$) to calculate the longitudinal velocity of the tractor semi-trailer ($\dot{x}$) by Sharp Rotary Encoder sensor (1); measure the longitudinal acceleration of the tractor semi-trailer ($\ddot{x}$) by MMA7361LC-XYZ sensor (2); weigh the un-sprung mass ($m_A$) and the sprung mass (m) with ULSTRALIM electronic balance (3). The diagram of the measurement system, signal reception and braking experimental result processing of the tractor semi-trailer is shown in Fig. 3 (Emery, 1998; Tung, 2016; Bouteldja et al., 2009).

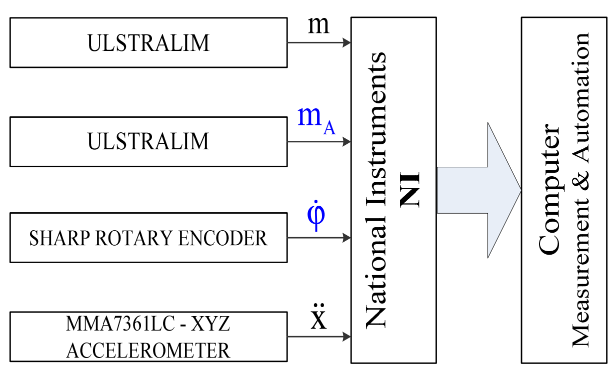


**Fig. 3.** Diagram of experimental system of braking force measurement

### *3.2. Experiment*

The object of the experiment is a 6-axle tractor semi-trailer, including a 3-axle FAW tractor and a 3-axle Tan Thanh semi-trailer. The weight of the tractor semi-trailer itself is 148 kN; the load of the tractor semi-trailer is 344 kN; the total weight of the tractor semi-trailer is 492 kN. The sensor installation diagram for measuring the parameters on the experimental tractor semi-trailer is shown in Fig. 4.

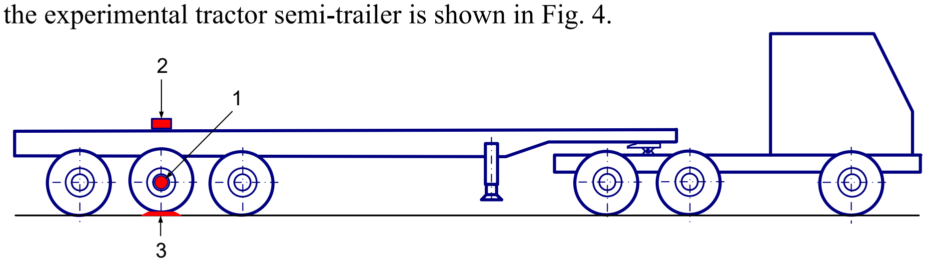


1. Sensor for measuring the wheel angular velocity; 2. Sensor for measuring longitudinal acceleration; 3. Weigh the axle weight

**Fig. 4.** Sensor installation diagram on the experimental tractor semi-trailer

The tractor semi-trailer was let to move steadily on the test road at a speed of 50 km/h and then the brake was applied to bring the tractor to a complete stop. At that time, the NI receiver and processor received signals from the sensors, processed the signals and sent them to the computer. Measurement & Automation software outputs were obtained for the test results. These results include the wheel angular velocity graph ($\dot{\varphi}$) as shown in Fig. 5; the longitudinal velocity graph of the tractor semi-trailer ($\dot{x}$) as shown in Fig. 6; the longitudinal grip coefficient graph ($\varphi_X$) as shown in Fig. 7 and the braking force graph $F_X$ as shown in Fig. 8.

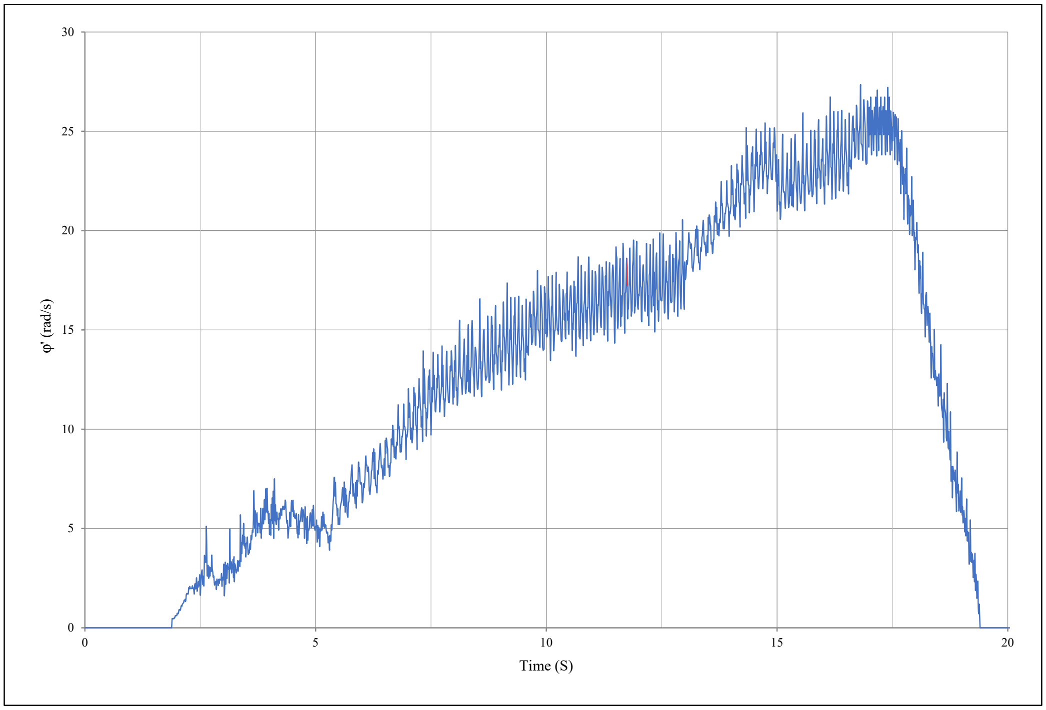


**Fig. 5.** Angular velocity graph of the wheel

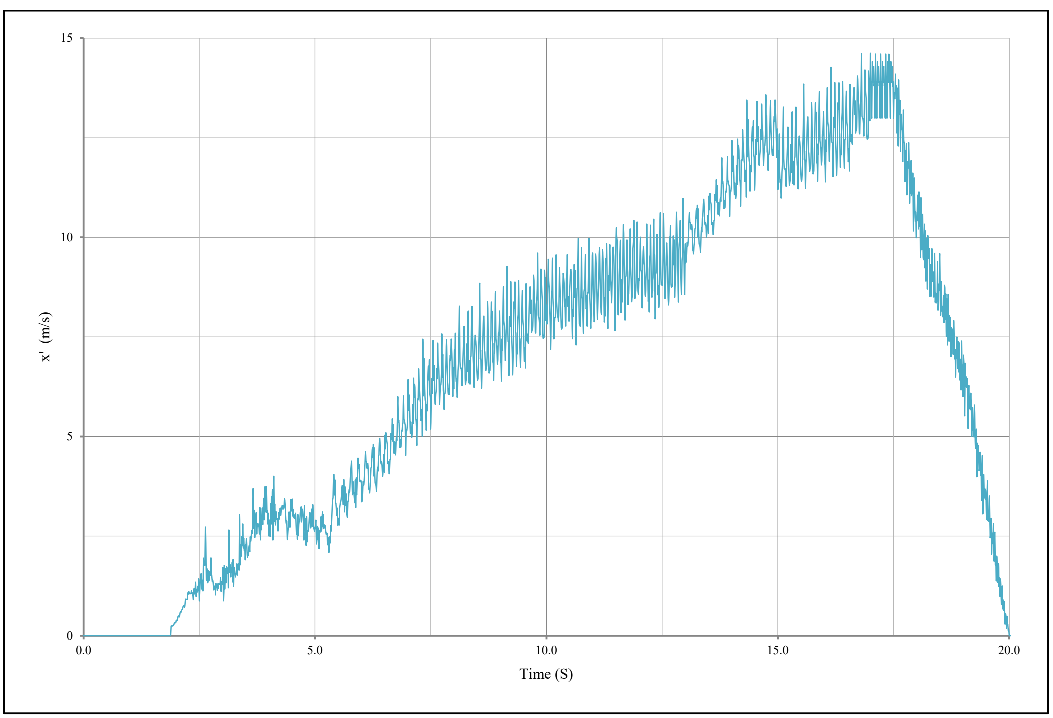


**Fig. 6.** Longitudinal velocity graph of the vehicle

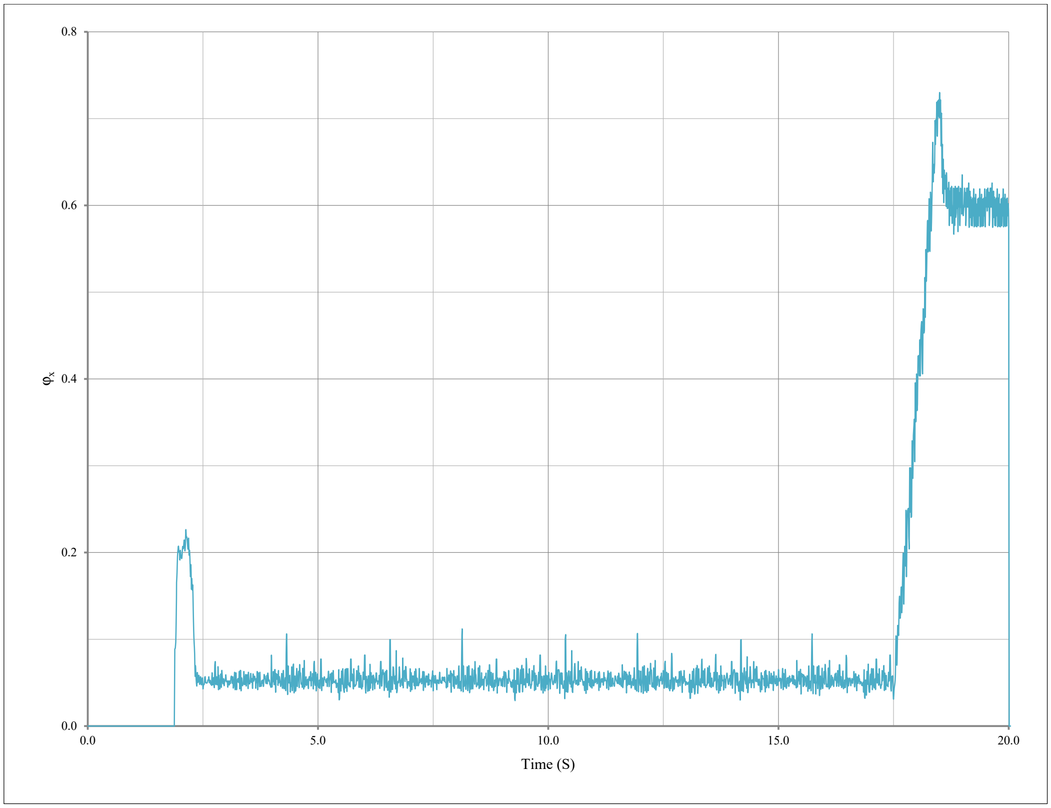


**Fig. 7.** Longitudinal grip coefficient graph

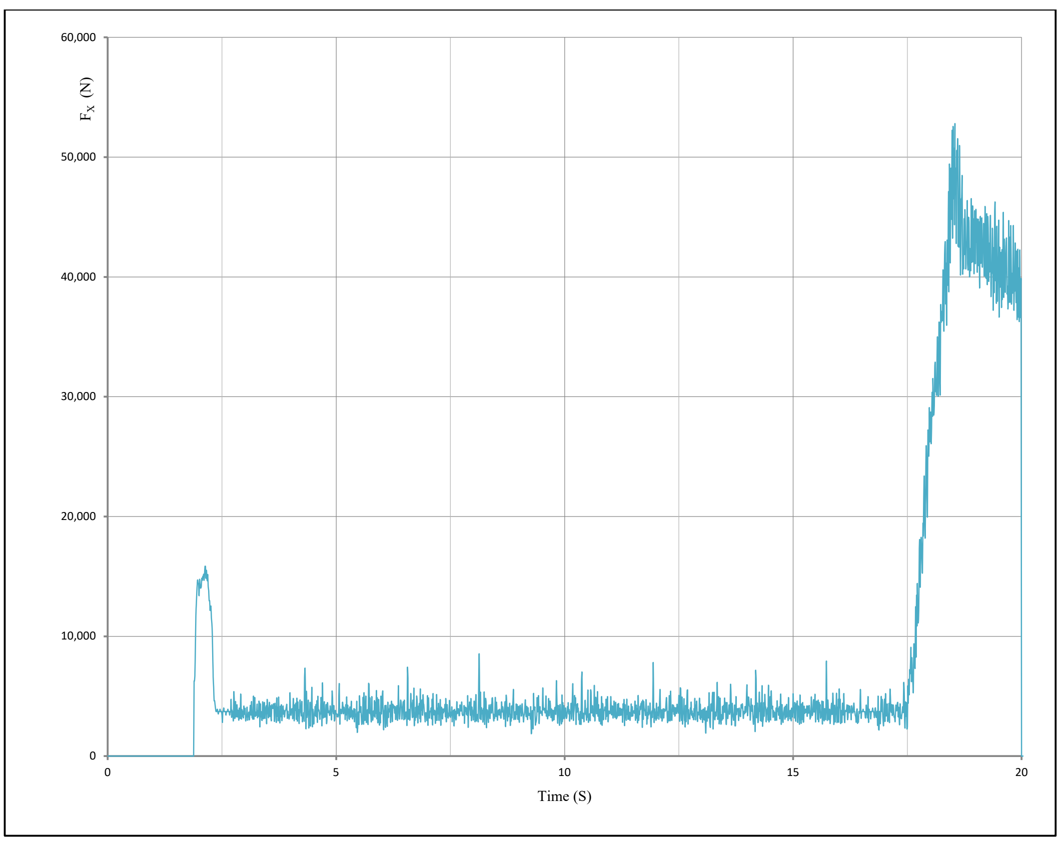


**Fig. 8.** Braking force $F_X$ graph

*3.3. Simulation*

Matlab-Simulink software was used to investigate the braking dynamics of a 6-axle tractor semi-trailer with the input conditions similar to the experimental conditions of the tractor semi-trailer on the actual road, and the simulation output was compared with the results obtained from the experiment (Keit, 2018). The tractor semi-trailer was surveyed at the speed of 50 km/h on the road with the grip coefficient $\varphi_{xmax}$=0.876; $\varphi_{xmin}$=0.736; the maximum braking force $F_{xmax}$=33013 N; brake at time t =0.5 s; the time from the start of the braking until the braking force reached its maximum value was 0.95 s. The simulation and experimental results of the wheel braking force of axle 5 are shown in Fig. 9. The survey showed that the average error between the simulation and experimental results of the braking force was 9.81%.

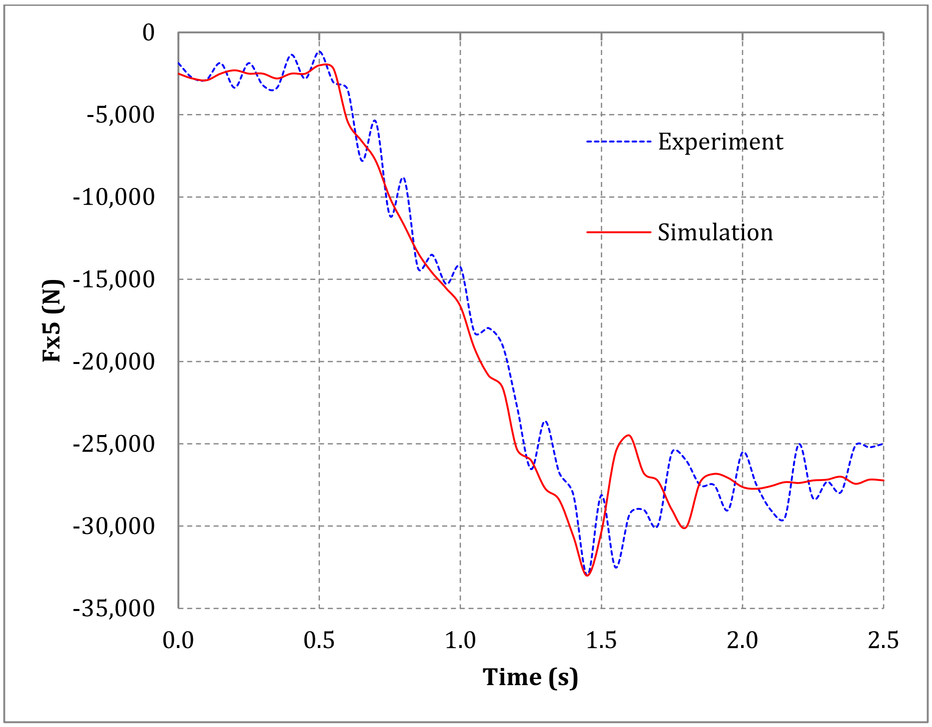


**Fig. 9.** The braking force of axle 5 wheel.

## 4. Conclusion

To determine the braking force of the tractor semi-trailer, a sensor that measures the longitudinal acceleration can be used. The design of this braking force measurement system is simple and at low cost. The system can be extended to measure the force applied to all wheels at the same time in different speed modes and road conditions. The measurement results reflect the physical state of the tractor semi-trailer quite accurately when moving on the road and when braking. The measurement results can be used to study the braking dynamics of the tractor semi-trailer as a basis for improving the braking system. In this paper, a method of setting up the braking force measurement system of the tractor semi-trailer on the road was illustrated and the braking dynamics model of the tractor semi-trailer was presented to investigate the braking force using Matlab-Simulink software. The results demonstrated that there is a good agreement between the simulation and experimental results of the tractor semi-trailer braking force.

## References

Bayan, F. P., Cornetto, A. D., Dunn, A., & Sauer, E. (2009). Brake timing measurements for a tractor-semitrailer under emergency braking. *SAE International Journal of Commercial Vehicles, 2*(2009-01-2918), 245-255.

Bouteldja, M., Jacob, B., & Dolcemascolo, V. (2009, April). Optimized design of weigh-in-motion multiple-sensors array by an energetic approach. In *International Conference on Heavy Vehicles HVParis 2008: Weigh-In-Motion (ICWIM 5)* (pp. 187-198). Hoboken, NJ, USA: John Wiley & Sons, Inc.

Chen, W., Xiao, H., Wang, Q., Zhao, L., & Zhu, M. (2016). *Integrated vehicle dynamics and control*. John Wiley & Sons.

Emery, L. (1998, October). Design and construction of a variable dynamic vehicle. In *16th International Technical Conference on the Enhanced Safety of VehiclesNational Highway Traffic Safety AdministrationTransport CanadaTransport Canada* (No. DOTHS808759).

Gäfvert, M., & Lindgärde, O. (2004). A 9-DOF tractor-semitrailer dynamic handling model for advanced chassis control studies. *Vehicle System Dynamics, 41*(1), 51-82.

GUAN, Z. W., XU, S. Y., YANG, L., & XU, H. G. (2004). Dynamics Analysis of Tractor-Semitrailer Braking Using Virtual Simulation Software ADAMS [J]. *Journal of Jilin Agricultural University, 6*.

Jazar, R. N. (2017). *Vehicle dynamics: theory and application*. Springer

Jazar, R. N. (2019). *Advanced vehicle dynamics*. Cham: Springer International Publishing.

Kiet P.T., Research on the vertical dynamic load of the tractor semi-trailer on the road (Doctoral thesis, Hanoi University of Science and Technology, 2018)

Lee, T. S., Chen, Y. H., & Chuang, C. H. (1999). Control for tractor-semitrailer vehicle systems: a Lyapunov minimax approach. *Dynamics and Control, 9*(1), 21-37.

Li, C., Li, X. H., & Wang, Z. (2014). Effect of load transfer of tractor-semitrailer on cornering braking stability. *Journal of Traffic and Transportation Engineering, 14*(2), 68-74.

Li, Y., Shi, Q., & Qiu, D. (2019). Parameter identification of tractor-semitrailer model under steering and braking. *Mathematical Problems in Engineering*, 2019.

Limpert, R. (1971). An investigation of the brake force distribution on tractor-semitrailer combinations. *SAE Transactions, 80*(1), 142-153.

Mitschke, M., & Wallentowitz, H. (1972). *Dynamik der kraftfahrzeuge* (Vol. 4). Berlin: Springer.

Rajamani, R. (2011). *Vehicle dynamics and control*. Springer Science & Business Media

Sampson, D. J. M. (2000). *Active roll control of articulated heavy vehicles* (Doctoral dissertation, University of Cambridge).

Suh, M. W., Park, Y. K., Kwon, S. J., Yang, S. H., & Park, B. C. (2000). A simulation program for the braking characteristics of tractor-semitrailer vehicle. *SAE transactions, 10*9(2), 540-550.

Tianjun, Z., & Changfu, Z. (2009, October). Modelling and active safe control of heavy tractor semi-trailer. *In 2009 Second International Conference on Intelligent Computation Technology and Automation (Vol. 2, pp. 112-115). IEEE.*

Tung N. T., *Research on braking efficiency on the roads with different grip coefficients of the tractor semi-trailer and proposed measures to reduce traffic accidents* (Doctoral thesis, Hanoi University of Science and Technology, 2016)

Tung, N. T., Huong, V. V., & Kiet, P. T. (2020). Experimental research on determining the vertical tyre force of a tractor semi-trailer. *International Journal of Modern Physics B*, *34*(22n24), 2040163.

Verma, V. S., Guntur, R. R., & Wong, J. Y. (1980). The directional behaviour during braking of a tractor/semi–trailer fitted with anti–locking devices. *International Journal of Vehicle Design, 1*(3), 195-220.

Vincent, R. J., & Krauter, A. I. (1973). Tractor-Semitrailer Handling: A Dynamic Tractor Suspension Model (No. 730653). SAE Technical Paper.

Werner, S. (2007). Dynamical Analysis of Vehicle Systems.

Zheng, H., Hu, J., & Ma, S. (2015). Research on simulation and control of differential braking stability of tractor semi-trailer (No. 2015-01-2842). SAE Technical Paper.

Zhiwei, G., Hongguo, X., Chunming, L., & Hongfei, L. (2005). Analysis of Brake Dynamics of Tractor-Semitrailer Combinations With Virtual Prototype Technology [J]. *Automobile Technology, 10*, 17-19.

Zhou, S. W., Zhang, S. Q., & Zhao, G. Y. (2011). Stability control on tractor semi-trailer during split-mu braking. *In Advanced Materials Research (Vol. 230, pp. 549-553). Trans Tech Publications Ltd.*

© 2021 by the authors; licensee Growing Science, Canada. This is an open access article distributed under the terms and conditions of the Creative Commons Attribution (CC-BY) license (http://creativecommons.org/licenses/by/4.0/).